13. R. Kelly, *Nucl. Instrum. Meth.*, **149**, 533 (1978).
14. Z. L. Liau, W. L. Brown, R. Homer, and J. M. Poate, *Appl. Phys. Lett.*, **30**, 626 (1977).
15. P. S. Ho, J. E. Lewis, H. S. Wildman, and J. K. Howard, *Surf. Sci.*, **57**, 393 (1976).
16. C. A. Anderson, *J. Mass, Spectrosc. Ion Phys.*, **2**, 61 (1969).
17. L. L. Chang and A. Koma, *Appl. Phys. Lett.*, **29**, 138 (1976).
18. P. M. Petroff, *J. Vac. Sci. Technol.*, **14**, 973 (1977).
19. J. A. VanVechten, "A Simple Man's Guide to Defect Thermochemistry" in Semiconductor Handbook, Vol. 3, S. Keller, Editor, North Holland (In press).
20. H. Kressel and M. Ettenberg, *J. Appl. Phys.*, **47**, 3533 (1976).

Microdistribution of Oxygen in Silicon

A. Murgai,*,[1] J. Y. Chi, and H. C. Gatos*

Department of Materials Science and Engineering, Massachusetts Institute of Technology, Cambridge, Massachusetts 02139

ABSTRACT

The microdistribution of oxygen in Czochralski-grown, p-type silicon crystals (75 mm in diameter and with a resistivity of 10 Ω-cm) was determined by using the SEM in the EBIC mode in conjunction with spreading resistance measurements. The crystals were heat-treated at 450°C to activate oxygen donors. When the conductivity remained p-type, (the oxygen donor concentration did not exceed the dopant concentration), bands of contrast were observed in the EBIC image which were found to correspond to maxima in resistivity, *i.e.*, to dopant compensation maxima and hence, to maxima in oxygen concentration. When at the oxygen concentration maxima the oxygen donor concentration exceeded (locally) the p-type dopant concentration, an inversion of the conductivity occurred. It resulted in the formation of p-n junctions in a striated configuration and the local inversion of the EBIC image contrast. A chemical etching procedure was developed, in conjunction with phase contrast microscopy, to delineate the n-type oxygen striations. By heat-treating silicon at 1000°C prior to the activation of oxygen donors, some silicon-oxygen micro-precipitates were observed in the EBIC image within the striated oxygen concentration maxima.

Variations in oxygen thermal donor concentration, activated by 450°C heat-treatment have been observed in Si (1-3) and determined by spreading resistance measurements (4, 5). The thermal donor concentration is proportional to the oxygen concentration and provides direct information on the microdistribution of oxygen. Such measurements, however, do not provide direct knowledge of the overall state of oxygen, *e.g.*, on the morphology of oxygen concentration variations, on oxygen clusters (6), and on precipitates (7-9). X-ray topography (10) has also been employed for the observation of oxygen concentration variations. This technique is at best qualitative in nature, as no quantitative relationship between topographic contrast and oxygen concentration is as yet available. In addition, the resolution of inhomogeneities by this technique is rather limited.

The electron beam induced current (EBIC) mode of scanning electron microscopy offers several advantages over the above characterization techniques. Dopant striations (11, 12), impurity precipitates (13), and other electrically active defects (14) can be simultaneously observed in the EBIC image with a relatively high resolution. Recently, the EBIC technique has been applied to the quantitative determination of dopant concentration variations (15), and employed in the study of impurity segregation (16). In addition, basic electronic parameters, such as minority carrier diffusion length, lifetime, and their variations (15, 16) can be readily determined with the EBIC technique.

In the present investigation, the EBIC technique has been applied to the study of microscale variations in oxygen concentration and their effects on p-type silicon crystals.

* Electrochemical Society Active Member.
[1] Present address: IBM Corporation, East Fishkill, New York 12533.

Experimental Procedure

Dislocation-free silicon crystals 75 mm in diameter and boron-doped to a level of about $5 \times 10^{14}/cm^3$ were pulled in the (100) direction from the melt. They were grown with a seed rotation of 5 rpm and a pulling rate of 75 mm/hr. The average oxygen concentration in the crystals, as determined from *IR* measurements (17). was found to be $1.8 \times 10^{18}/cm^3$.

All measurements were made on (100) longitudinal slices, 0.5 mm thick. The slices were heat-treated at 450°C for 50 hr, lapped, and polished with Syton HT. After cleaning with an organic solvent and etching in $HF + HNO_3 + CH_3COOH$, a 0.5 μm Al layer (2×2 cm) was deposited on these slices to obtain a semiconductor-metal Schottky barrier (collecting field).

Impact traces of spreading resistance probes were introduced (at 5 or 25 μm intervals) on the Schottky diode to serve as location markers (see also below). EBIC measurements were subsequently conducted in the region of the impact traces with an electron beam accelerating voltage of 35 kV. At the above accelerating voltage the electron range, *R*, lies outside the depletion width of the Schottky barrier for 10 Ω-cm Si (18). The experimental arrangement for the EBIC measurements and imaging is indicated schematically in Fig. 1.

Following EBIC measurements, the metal layer was stripped from the slice with concentrated HCl. Longitudinal variations in the thermally activated donor concentration (introduced by the 450°C heat-treatment) were determined from spreading resistance measurements (at 5 μm intervals) carried out near and parallel to the impact traces introduced earlier, the traces were still present after the metal layer was stripped. The spreading resistance measurements were made employing both polarities of the d-c bias between the two probes. From such measurements, the presence of any

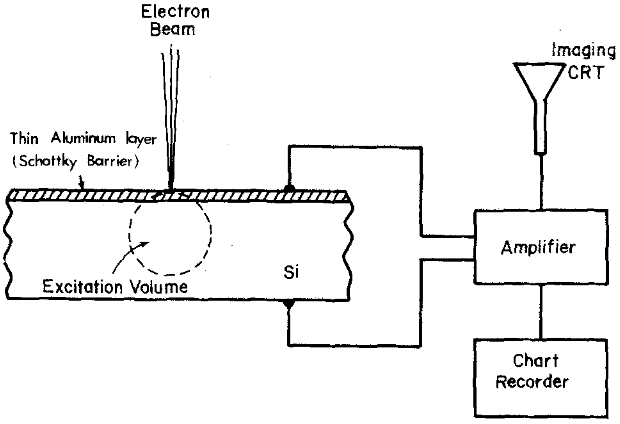

Fig. 1. Schematic diagram of experimental arrangement for EBIC measurements.

p-n junctions formed during the 450°C heat-treatment was readily determined.

The slices were subsequently heat-treated at 700°C for 1 hr to eliminate the oxygen thermal donors (1-3); following this heat-treatment EBIC and spreading resistance measurements were repeated in the identical regions using the impact traces of the spreading resistance probe as reference.

In certain instances, the slices were heat-treated at 1000°C for 12 hr in ultrahigh purity argon prior to the 450°C heat-treatment. The 1000°C heat-treatment induces some form of silicon-oxygen precipitation in the slices as confirmed by *IR* measurements.

Results and Discussion

Oxygen striations—compensation.—Following the 450°C heat-treatment, the presence of oxygen striations is seen in Fig. 2 for a longitudinal slice cut 0.5 mm from the periphery of a typical 75 mm diam. The oxygen striations are seen in the EBIC image [Fig. 2(a)] as bright bands and the corresponding variations in the normalized EBIC and resistivity (as determined from spreading resistance measurements at 5 μm intervals) are shown in Fig. 2(a) and (b), respectively.

As can be seen from Fig. 2(a) and (b), there is direct spatial correspondence of the variations in the normalized EBIC and resistivity; the large variations (exceeding a factor of 10) in resistivity following the 450°C heat-treatment reflect corresponding variations in the oxygen thermal donor concentration (and, hence, in the oxygen concentration), since variations in the boron acceptor concentration are less than 12% (see below); the oxygen striations in the EBIC image, Fig. 2(a), manifested as bright bands, correspond to the maxima in resistivity [Fig. 2(b)] which in turn correspond to oxygen concentration maxima. Maxima in resistivity are expected to coincide with maxima in oxygen thermal donors, since the higher the concentration of the thermal donors, the higher the compensation of the p-type dopant and hence the higher the resistivity (provided the concentration of thermal donors does not exceed the concentration of the acceptors).

In the regions of maximum resistivity, the space charge region (depletion width) of the Schottky diode is significantly increased. For resistivities of about 200 Ω-cm the depletion width is several microns but well within the excitation volume of a 35 keV electron beam. Accordingly, the collection efficiency of the excess carriers is enhanced in these regions of the oxygen concentration maxima and consequently appear as bright bands in the EBIC image.

As seen in Fig. 2(a) and 2(b), the width of the EBIC maxima (*e.g.*, the width at half the maximum value) is larger than that of the resistivity maxima. This result is apparently due to interference effects of the electric fields resulting from the resistivity variations.

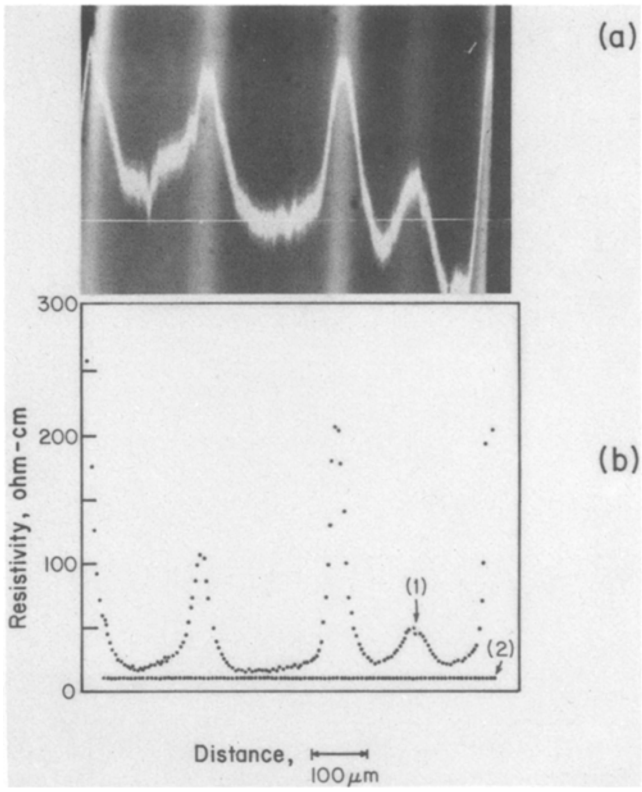

Fig. 2. (a) EBIC image and superimposed EBIC tracing taken along indicated line on a sample cut near crystal periphery (see text). (b) Resistivity profile as determined by spreading resistance measurements at 5 μm intervals along the line indicated in EBIC image after 450°C heat-treatment, curve 1; profile taken prior to 450°C heat-treatment, curve 2; small variations of boron concentration are not visible on this scale.

Since the spacing of the spreading resistance impact traces in the EBIC image is 5 μm, it is seen from a comparison of the resistivity and the normalized EBIC that the linear resolution attained by the EBIC technique in the present case is about 10 μm.

It has been found that heat-treatment of Si at 700°C eliminates oxygen thermal donors (1-3). Consistent with this finding, after heat-treatment of the slices studied above at 700°C for 1 hr, their EBIC images exhibited no bands. The normalized EBIC and resistivity measurements carried out in the same regions as discussed above exhibited small variations.

These variations are due to B-dopant fluctuations which in 10 Ω-cm Si are about 12% [Fig. 2(b)]. These B-dopant fluctuations are not resolved in the EBIC image.

Oxygen striations and overcompensation.—Longitudinal slices cut 1 cm from the crystal periphery were also investigated. They were also treated at 450°C for 50 hr and prepared for EBIC and spreading resistance measurements as discussed above.

The EBIC image of one of these slices is shown in Fig. 3(a). Spreading resistance measurements were carried out at 5 μm intervals, 20 μm below the horizontal impact trace markers which are spaced 25 μm apart and are clearly shown in the EBIC image. Dark bands are seen in the EBIC image which correspond to resistance minima in Fig. 3(b). These dark bands (regions of low collection efficiency of excess carriers) correspond to oxygen striations in which the donor concentration exceeds the concentration of the p-type dopant forming striated n-type regions (see below). Since the donor concentration is a direct function of the oxygen concentration (2), the presence of n-type regions only in the slices cut 1 cm away from the periphery shows that the mean oxygen concentration is higher

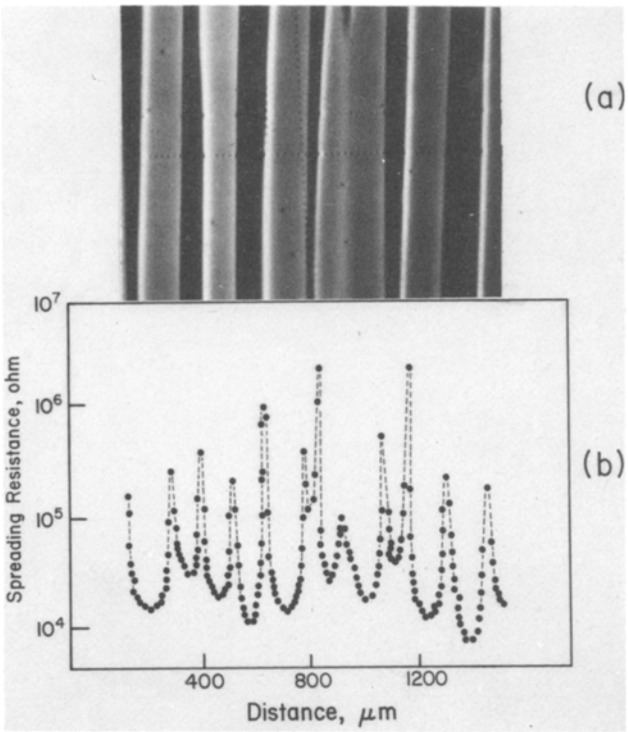

Fig. 3. (a) EBIC image on sample cut away from crystal periphery. Reference impact traces are clearly visible. (b) Spreading resistance profile taken at 5 μm intervals, 20 μm below horizontal line of reference tracers.

away from the periphery than near the periphery of the crystals. The bright bands (adjacent to the dark bands) in Fig. 3(a) correspond to regions of maxima in compensation as in the case of Fig. 2(a) but not to maxima in oxygen concentration.

The conductivity type within the dark bands was determined as follows: employing a two-probe spreading resistance measurement arrangement, measurements were carried out at 5 μm intervals with one of the probes positioned at all times on a dark band as shown in Fig. 4(a). As shown in Fig. 4(b) with the probe on the dark band having a negative polarity the measured resistance was about $8 \times 10^5 \Omega$. When the bias was reversed the resistance increased by about three orders of magnitude. Thus, there is a p-n junction at the boundary of each dark band and the adjacent bright band; the dark band is n-type and corresponds to a region overcompensated by thermal oxygen donors. After a 700°C heat-treatment (which eliminates the thermal oxygen donors) no dark bands in the EBIC image nor pronounced variations in resistance were present; this result confirms that the n-type regions (dark bands) are the result of oxygen donors.

Chemical etching.—It was found that oxygen striations can be conveniently revealed by chemical etching when they form n-type regions in p-type silicon. The etchant found suitable for this purpose is 20 parts $CH_3COOH + 3HNO_3 + 1HF$. An interference contrast photomicrograph of the slice etched for 20 min (after the metal layer was removed) is shown in Fig. 5. The area depicted in this figure is identical to that in the EBIC image of Fig. 3(a). It is seen that the striations in Fig. 5 correspond exactly to the dark band in Fig. 3(a). The bright bands (region of compensation maxima) could not be revealed by etching. Thus, a bright band in location D of Fig. 3(a) does not appear in Fig. 5; similarly, no oxygen striations could be revealed by etching on slices cut near the crystal periphery which correspond to oxygen concentration maxima but lead to maxima in compensation as in the case shown in Fig. 2(a).

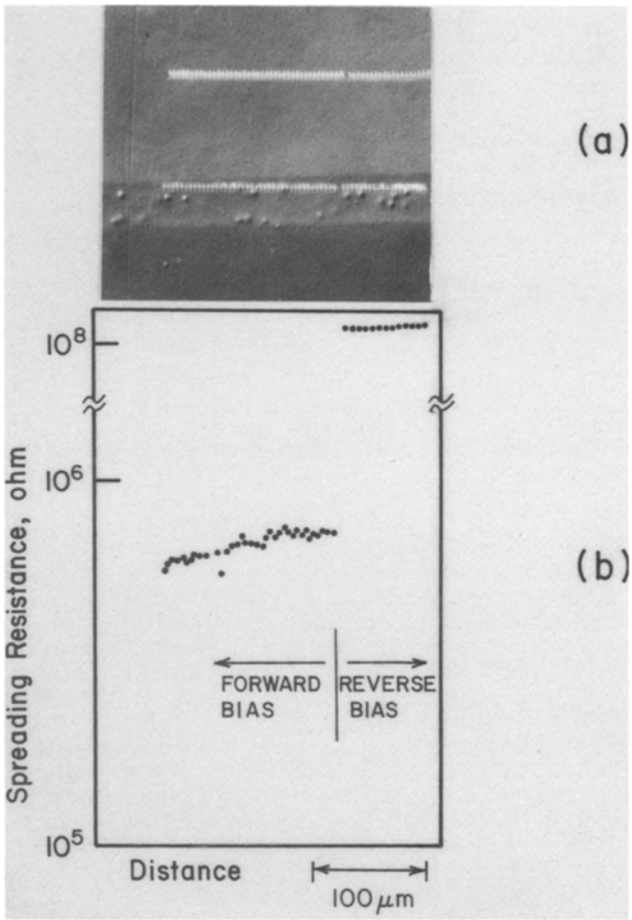

Fig. 4. (a) Optical photomicrograph of chemically etched surface (see text) showing impact traces of two-probe spreading resistance measurements. Traces of one probe are within dark band measurements of EPIC image (Fig. 2) while traces of other probe are outside dark band (for convenience the dark band is shown in the horizontal position). (b) Spreading resistance measured with both polarities of the d-c bias. Polarity was reversed at the discontinuity of the impact traces.

SiO_2 precipitation.—Silicon slices heat-treated at 1000°C for 12 hr prior to heat-treatment at 450°C (for activating thermal donors) exhibited silicon-oxygen precipitation (19). An EBIC image of a slice cut from near the periphery of the crystal is shown in Fig. 6(a). It is seen that within the bright bands [corresponding to maxima in resistivity, Fig. 6(b); compare also with Fig. 2] there are dark spots with low excess carrier

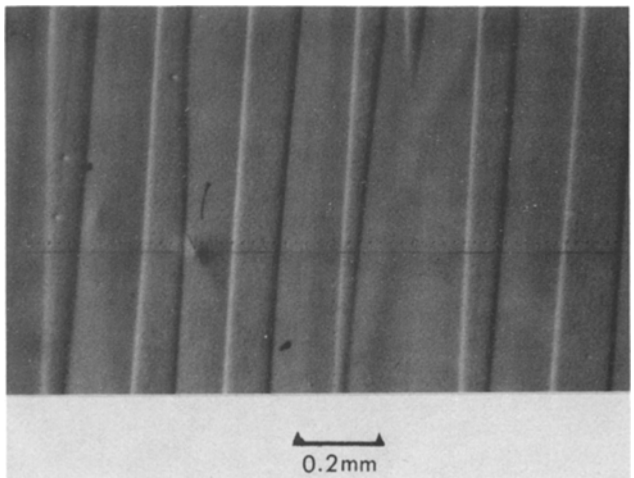

Fig. 5. Optical photomicrograph of chemically etched sample showing the identical region as EBIC image of Fig. 3(a).

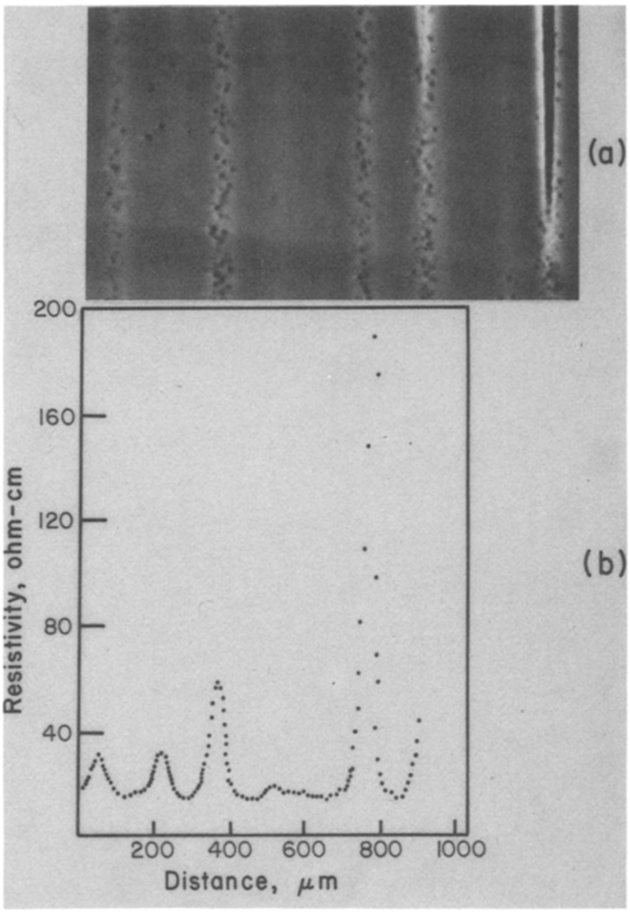

Fig. 6. (a) EBIC image of sample heat-treated at 1000°C prior to a 450°C heat-treatment. (b) Resistivity as determined from spreading resistance measurements.

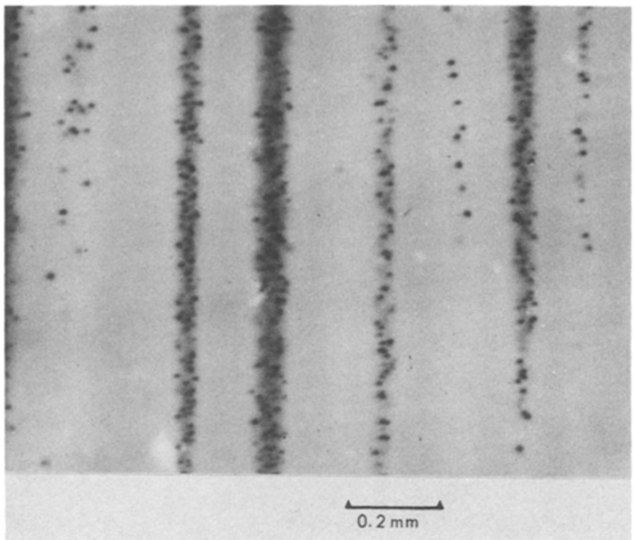

Fig. 7. EBIC image of sample heat-treated at 700°C after heat-treatments at 1000° and 450°C.

collection efficiency which are associated with microprecipitates (and related loops and stacking faults). On the right-hand side of the EBIC image there are two dark bands, corresponding to overcompensated, n-type regions, which also contain microprecipitates. Apparently, the 12 hr 1000°C heat-treatment causes only partial precipitation of oxygen, since a subsequent 450°C heat-treatment leads to the formation of thermal oxygen donor striations (bright and dark bands in the EBIC image). The fact that the microprecipitates are associated with oxygen was confirmed by *IR* transmission measurements which showed that after the 1000°C, and prior to the 450°C, heat-treatment the interstitial oxygen content in Si was reduced.

As in the cases discussed earlier, heat-treatment at 700°C eliminates the oxygen donor striations, however, the microprecipitates can still be seen (Fig. 7).

Although the detailed nature of the micro-defects generated by these precipitates will not be discussed in the present communication, it should be pointed out that the morphology of the etch pits, revealed by the Sirtl etchant, was found to correspond to that associated with stacking faults as discussed in the literature.

Summary and Conclusions

The distribution of oxygen in Czochralski-grown p-type silicon was studied by scanning electron microscopy in the EBIC mode in conjunction with spreading resistance measurements. A linear resolution of about 10 μm was achieved in the determination of oxygen distribution. Through generation of thermal oxygen donors (by heat-treating at 450°C) it was found that oxygen is distributed in a striated pattern. At the oxygen concentration maxima, maxima in dopant compensation occur, provided the thermal donor concentration does not exceed the p-type dopant concentration. These compensation maxima appear as bright bands in the EBIC images (high collection efficiency regions of excess carriers) and exhibit high resistivity as determined by spreading resistance measurements. If at the oxygen concentration maxima the thermal donor concentration exceeds that of the p-type dopant, then dopant overcompensation takes place. These regions become n-type and appear as dark bands (low collection efficiency regions of excess carriers) adjacent to bright bands (highly compensated regions). The boundaries of these regions constitute p-n junctions which could be individually characterized with a two-probe spreading resistance arrangement.

Oxygen precipitates resulting from a heat-treatment at 1000°C were found to be distributed in a striated pattern and within the regions of oxygen concentration maxima. Unlike the thermal oxygen donors the precipitates were not eliminated by prolonged heat-treatment at 700°C.

Etching with a mixture of 20 parts CH_3COOH + $3HNO_3$ + 1HF was found to delineate conveniently and accurately the oxygen striations in the cases where the oxygen donors overcompensate the p-type dopant (dark bands in the EBIC image); this etchant also revealed oxygen precipitates. However, the oxygen striations could not be revealed by etching in the cases where the oxygen donors do not overcompensate the p-type dopant.

The EBIC technique employed in the present study, in conjunction with spreading resistance measurements, is well suited for quantitative study of the microsegregation of oxygen in silicon and its quantitative interactions with electronic phenomena and defect structure. It should be finally noted that controlled formation of p-n patterns through controlled incorporation of oxygen in silicon could be advantageously employed for photovoltaic cell and other device applications.

Acknowledgment

The authors are grateful to the International Business Machines Corporation and the National Aeronautics and Space Administration for financial support and to Dr. W. A. Westdorp for stimulating discussions.

Manuscript submitted April 24, 1979; revised manuscript received Oct. 29, 1979.

Any discussion of this paper will appear in a Discussion Section to be published in the December 1980 JOURNAL. All discussions for the December 1980 Discussion Section should be submitted by Aug. 1, 1980.

Publication costs of this article were assisted by the Massachusetts Institute of Technology.

REFERENCES

1. C. S. Fuller, J. A. Ditzenberger, N. B. Hannay, and E. Buehler, *Phys. Rev.*, **96**, 833 (1954); *Acta Metall.*, **3**, 97 (1955).
2. W. Kaiser, H. L. Frisch, and H. Reiss, *Phys. Rev.*, **112**, 1546 (1958).
3. V. N. Mordkovich, *Sov. Phys. Solid State*, **6**, 654 (1964).
4. T. Abe, K. Kikuchi, and S. Shirai, in "Semiconductor Silicon 1977," H. R. Huff and E. Sirtl, Editors, p. 95, The Electrochemical Society Softbound Proceedings Series, Princeton, N.J. (1977).
5. A. Murgai, H. C. Gatos, and W. A. Westdorp, *This Journal*, **126**, 2240 (1979).
6. J. R. Patel and B. W. Batterman, *J. Appl. Phys.*, **34**, 2716 (1963).
7. W. Kaiser, *Phys. Rev.*, **105**, 1751 (1957).
8. D. M. Maher, A. Staudinger, and J. R. Patel, *J. Appl. Phys.*, **47**, 3813 (1976).
9. T. Y. Tan and W. K. Tice, *Philos. Mag.*, **34**, 615 (1976).
10. G. H. Schwuttke, *J. Appl. Phys.*, **33**, 2760 (1962).
11. A. J. R. de Kock, S. D. Ferris, L. C. Kimerling, and H. J. Leamy, *J. Appl. Phys.*, **48**, 301 (1977).
12. C. N. Varker and K. V. Ravi, in "Semiconductor Silicon 1973," H. R. Huff and R. R. Burgess, Editors, p. 670, The Electrochemical Society Softbound Proceedings Series, Princeton, N.J. (1973).
13. L. C. Kimerling, H. J. Leamy, and J. R. Patel, *Appl. Phys. Lett.*, **30**, 217 (1977).
14. H. J. Leamy, L. C. Kimerling, and S. D. Ferris, in "Scanning Electron Microscopy 1976," Part IV, p. 526, ITT Research Institute, Chicago (1976).
15. J. Y. Chi and H. C. Gatos, *J. Appl. Phys.*, **50**, 3433 (1979).
16. J. Y. Chi, A. Murgai, and H. C. Gatos, Unpublished.
17. 1977 Annual Book of ASTM Standards, Part 43, ASTM, Philadelphia (1971).
18. T. E. Everhart and P. H. Hoff, *J. Appl. Phys.*, **42**, 5837 (1971).
19. K. H. Yang, P. Anderson, and H. Kappert, *Appl. Phys. Lett.*, **33**, 225 (1978).

The Influence of Preparation on Semiconducting Rutile (TiO_2)

L. A. Harris and R. Schumacher

General Electric Corporate Research and Development, Schenectady, New York 12301

ABSTRACT

Three processes for doping rutile crystals, vacuum reduction, hydrogen reduction, and electrochemical hydrogen loading are considered. The mechanisms by which n-type conductivity is produced, the relative disorder in the crystal, and the effects on photoelectrochemical behavior are compared for these different processes.

Rutile has received a great deal of attention as an electrode in photoelectrochemical studies. It is usually made conducting by some form of reduction such as heating in vacuum, in hydrogen, or by introducing an appropriate impurity such as fluorine. More recently it has been shown that conductivity can be induced by electrochemically charging the TiO_2 with hydrogen at room temperature (1, 2). It is the purpose of this note to suggest that the materials produced by these doping processes have different chemical and physical structures that influence their electronic behavior as photoelectrochemical electrodes.

Vacuum Reduction

To produce conductivity in a TiO_2 crystal by vacuum treatment, temperatures exceeding about 700°C are required (3). It has been established that the crystal loses weight during this treatment due to the loss of water and oxygen (4, 5). The oxygen vacancies so formed leave some of the Ti atoms in the 3+ state and these can readily act as donors, providing electrons to the conduction band. Relatively high temperatures are required because bonds between an O atom and the remainder of the lattice must be broken so that O can diffuse out of the crystal.

Some disorder is introduced by this reduction process, and interstitial Ti atoms have been detected by channeling experiments (6). As oxygen content is decreased the crystal rearranges itself to accommodate the various Magneli phases by introducing shear planes or grain boundaries where extra titanium atoms are located (7-9).

The disorder in the crystal manifests itself in the photoelectrochemical characteristics. The poor response to longer wavelengths of light which are absorbed deep in the crystal and the low quantum efficiency are indicative of short hole diffusion lengths due to a high density of bulk recombination sites (3).

Vacuum reduction appears to be the only process by which hydrogen, evidenced by OH absorption peaks in the infrared spectrum, can be removed from these crystals (10, 11).

Hydrogen Reduction

If rutile is heated in hydrogen, conductivity can be induced at temperatures roughly 200°C lower than those required to induce comparable conductivities by heating in vacuum (3). The presence of hydrogen in the crystal is shown by the appearance of OH absorption peaks, indicating that the hydrogen is bound to O atoms of the lattice. There are usually two peaks, one at 3276 cm^{-1} and a smaller one at 3323 cm^{-1} (10, 11). One might speculate that the peak at 3276 cm^{-1} is due to H bonded between two lattice O atoms (10) and that the peak at 3323 cm^{-1} is due to H bonded to a single lattice O atom. These peaks are not to be confused with those due to surface-adsorbed OH which occur at 3620 and 3680 cm^{-1} (12). This interpretation is consistent with the appearance of a third peak at 3345 cm^{-1} in samples etched in molten NaOH (Fig. 1). This third peak, attributable to interstitial OH groups is removed by heating in H_2 but not by heating in O_2.

Recent observations of the diffusion of tritium in TiO_2 agree with computed values under the assumption that the tritium is bonded to lattice O atoms (13, 14). In contrast to the vacuum reduced case no O atoms need be lost from the crystal and the crystal order is not so seriously disturbed. We may think of the conductivity as being produced by the change of divalent O ions to monovalent OH ions, thus leaving Ti^{3+} ions

Key words: semiconductor electrodes, photoelectrochemistry, hydrogen, doping.